

THE ROLE OF FIELD COUPLING IN NANO-SCALE CELLULAR NONLINEAR NETWORKS

WOLFGANG POROD, GYÖRGY CSABA, and ÁRPÁD CSURGAY¹

*Center for Nano Science and Technology, Department of Electrical Engineering
University of Notre Dame, Notre Dame, Indiana 46556*

Porod@nd.edu

In this paper we review some of the newly-emerging nanotechnologies, including new ways of imaging and manipulating matter on the nanometer scale. Electronic devices based on metallic and magnetic nanoscale dots and on molecular structures have been suggested, however, no technologically viable architecture for nanoelectronic circuit integration has emerged. The natural architecture on the nanoscale is near-neighbor cellular networking, and promising alternative ways of integrating nanodevices by field coupling, i.e. either by Coulomb coupling or by magnetic coupling are being explored. In this paper, new architectures for such field-coupled nanocircuits will be reviewed.

1 Introduction

Recent studies, and many examples provided by nature, show that the laws of physics present no barriers to reducing the size of data storage cells and logic gates, until basic components are the size of atoms or molecules. In the deep-submicron and nanoscale regime, the physics of devices challenges our classical design methodology. Quantum effects emerge and frequently they hold dominant sway. With the advent of scanning probe microscopy the nanometer scale has become visible, and we have begun to master the manipulation of nanoscale objects as well [1].

For the first time in the history of science, atomic force microscopy (AFM) and scanning tunneling microscopy (STM) brought within reach single atoms and molecules on a surface [2].

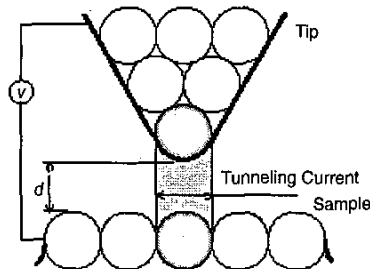


Figure 1. Scanning Tunneling Microscope (STM). The tunneling current is measured as the tip scans over the surface of the sample.

¹ On leave from the Budapest University of Technology and Economics, Department of Electromagnetic Theory, Budapest, Hungary

Figure 1 shows a schematic drawing of a Scanning Tunneling Microscope (STM). When the tip is brought within about 1 nm (10 Å) of the sample, electrons from the sample begin to "tunnel" through the 10 Å gap into the STM tip or vice versa, depending upon the sign of the applied bias voltage. The resulting tunneling current varies with tip-to-sample spacing, and it is the signal used to create an STM image. For tunneling to take place, both the sample and the tip must be conductors or semiconductors. STMs cannot image insulating materials, but an atomic force microscope (AFM) can. Note that the image of the tunneling current does not map the topography of the sample, but the tunneling current corresponds to the electronic density of states at the surface. STMs sense the number of filled or unfilled electron states near the Fermi surface, within an energy range determined by the bias voltage. It was headline news when researchers first picked up a single atom by an STM tip, moved it, and by repeating this process, they were able to write letters or draw figures on a surface.

The atomic force microscope (AFM) probes the surface of a sample with a sharp tip, a couple of microns long and often less than 10 nm in diameter. The tip is located at the free end of a cantilever that is 100 to 200 μm long. Forces between the tip and the sample surface cause the cantilever to bend, or deflect. A detector measures the cantilever deflection as the tip is scanned over the sample. The measured cantilever deflections allow a computer to generate a map of surface topography. It is remarkable that a tip of diameter 10 nm is able to map a surface with a resolution smaller than 0.01 nm, which is smaller than the size of an atom [3].

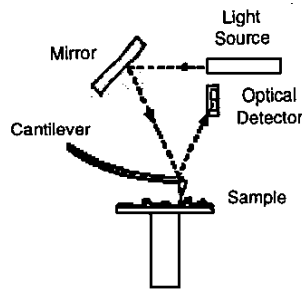


Figure 2. Atomic Force Microscope (AFM). Forces between the tip and the surface of the sample are sensed through the bend or deflection of a cantilever

Most AFMs currently on the market detect the position of the cantilever with optical techniques. Figure 2 shows that a laser beam bounces off the back of the cantilever onto a position-sensitive photo-detector. As the cantilever bends, the position of the laser beam on the detector shifts. The ratio of the path length between the cantilever and the detector to the length of the cantilever itself produces a mechanical amplification. As a result, the system can detect sub-angstrom vertical movement of the cantilever tip. Other methods of detecting cantilever deflection rely on optical interference. It is also possible to fabricate the cantilever from a piezo-resistive material so that its deflection can be detected electrically. In piezo-resistive materials, strain from mechanical deformation causes a change in the material's resistivity.

It is possible to image a surface by AFM without contacting it. Non-contact AFM (NC-AFM) is a vibrating cantilever technique in which an AFM cantilever is vibrated

near the surface of a sample. It is desirable because it provides a means for measuring sample topography with little or no contact between the tip and the sample. Like contact AFM, non-contact AFM can be used to measure the topography of insulators and semiconductors as well as electrical conductors. In non-contact mode, the system vibrates a cantilever near its resonant frequency (typically a few 100 kHz) with amplitude of a few tens of angstroms. Then it detects changes in the resonant frequency or vibration amplitude as the tip comes near the sample surface. The sensitivity of this detection scheme provides sub-angstrom vertical resolution in the image.

If the tip is coated with a ferromagnetic thin-film, images of the spatial variation of magnetic forces on a sample surface can be viewed. The system operates in non-contact mode, detecting changes in the resonant frequency of the cantilever induced by the magnetic field's dependence on tip-to-sample separation.

Cantilevers and their tips are critical components of an atomic force microscope system because they determine the force applied to the sample and the ultimate lateral resolution of the system. Integrated tip and cantilever assemblies can be fabricated from silicon using photolithography. More than 1,000 tip and cantilever assemblies can be produced on single silicon wafer [3].

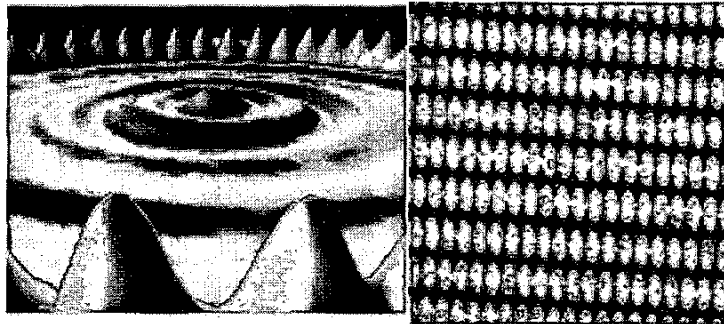


Figure 3 Scanning Tunneling Microscope (STM) image of a copper surface with a circular ring of iron atoms on it, and Atomic Force Microscope (AFM) image of an array of patterned nanomagnets.

Nanoelectronic fabrication techniques, enabled by STM and AFM capabilities, offer the promise of ultra-low power and ultra-high integration density. Several device structures have been proposed and realized experimentally, yet the main challenge remains the organization of these devices into new circuit architectures. Classical wiring imposes severe limitations and in many cases destroys dynamics. Nature utilizes field coupling to assemble matter, and the chemical bond is field coupling. Intermolecular forces are either Coulombic or magnetic (spin) forces. The natural 'architecture' is 'cellular', though not regular. The degree of freedom is limited by the laws of physics and the nature of forces between devices.

In this paper, we investigate the idea of physical device-device interactions in the form of field coupling to provide local connectivity. We focus both on Coulomb-coupled

molecular nanostructures and quantum-dot arrays [4 – 9], as well as magnetically-coupled arrays of nano-magnet structures [10 – 12].

Cellular Nonlinear Network (CNN)-type architectures [13 – 14] for nanostructures are motivated by the following considerations: On the one hand, locally-interconnected architectures appear to be natural for nanodevices where some connectivity may be provided by direct physical device-device field coupling. On the other hand, large-scale CNN (which are desirable for applications such as image processing) will require the use of nanostructures since the required integration densities are beyond what can be achieved by scaling conventional CMOS devices [15].

2 Field-Coupled Nanocircuits

In electronics, three ways of interconnecting nanodevices have been suggested so far. Metal-contacted devices in the macro- and meso-scale (10 to 100 nanometers and above), such as nano-transistors, resonant tunneling devices (RTD's), and metal-dot single-electron transistors (SET's), can be interconnected with wires. As long as each device has metal contacts, i.e. they are all embedded into a "heat bath," conventional interconnections with wires are possible. In this case, circuit dynamics obeys the conventional Kirchhoff's laws, which are a consequence of the basic conservation of charge and energy. Alternatively, nanodevices which are not metal contacted, e.g. quantum-dot arrays and artificial atoms and molecules, can be coupled either by inter-device transport, or by fields (electric and/or magnetic). In the case of wiring and inter-device electronic transport, the flow of current generates unavoidable dissipation of energy and also contributes to the well-known interconnect bottleneck.

An alternative approach to device integration is the use of electromagnetic field interactions between the devices, such as coupling by Coulombic or by magnetic forces. This approach becomes more natural as devices come closer to each other (increasing packing densities) and it also significantly reduces unwanted power dissipation. Field coupling can transfer energy between devices by exciton transfer, electron transfer, proton transfer, and also by the magnetic forces between spins and magnetic domains.

For the case of metal-contacted devices, we can rely on the fact that metal contacts are 'equipotential-' and 'thermal bath-' type; because of the physics of these interconnection types, the Kirchhoff equations at the nodes are satisfied. Device modeling is still an art. Nevertheless, the circuit paradigm offers a solid theoretical foundation for the analysis and design of nanocircuits composed of metal-contacted devices.

Note that field coupling is different. Even if the coherent quantum dynamics is restricted to the internal dynamics of the devices, one needs to introduce 'quasi-charges' and 'quasi-voltages' which formally satisfy Kirchhoff-type equations. In previous work, we have demonstrated this approach by relying upon the conservation of charge and energy [4]. We have introduced circuit models which include exciton and electron dynamics, proton switches, and even the case of proton 'tunneling'. We have shown that nanodevice dynamics can be described as a mixed quantum-classical dynamics with state vectors composed of 'coherence vectors' and of the position and momenta of the non-tunneling 'nuclei' [4].

There is a wide variety of nanosystems that might serve as “building blocks” of field-coupled QCA-type [6] nanocomputers. In particular, nanomagnet arrays are emerging as a promising realization possibility. Due to the relatively strong interaction energy (typically few hundred kT between few-ten nm size dots), these structures exhibit robust, room temperature operation. The feasibility of a line consisting of magnetically-coupled dots has already been proposed and experimentally verified [10]. We have applied quantum micromagnetics to model arrays of nanomagnets, to simulate their dynamics and to propose circuits for nanocomputing [11], which will be discussed below.

The circuit paradigm can serve as a tool for the 'analysis' of a nanosystem, by providing a hierarchy of models. If we would like to 'design' a system we start from our expectations on the results of simulation. We prescribe the 'behavior' and we are looking for a circuit with specified parameters, and for the geometry and material properties of the circuit. We are looking for the solution of an 'inverse' (synthesis) problem.

If both metal-contacted and field-coupled devices are to be integrated into the same circuit, the physical interfaces between the two types of devices can be represented as classical electromagnetic circuits. The boundary condition on the side of the metal-contacted devices are defined by the metal contacts (voltages and currents) and on the side of the field-coupled devices by the electric or magnetic fields generated by the nanodevice. We have developed equivalent-circuit representations for circuits composed of both metal-contacted and field-coupled nanodevices. Thus, the circuit paradigm can be applied to build device models, to simulate, and to aid the design of large-scale nanoelectronic integrated circuits.

3 Equivalent-Circuit Models for Field-Coupled Nanodevices

In this section, we will outline the development of equivalent-circuit models for field-coupled nanostructures. As schematically shown in Figure 4, the individual device (molecule) is dissipatively coupled to a heat bath, it is exposed to external forces, such as clocking circuitry, and it couples to its neighbors through electric or magnetic fields.

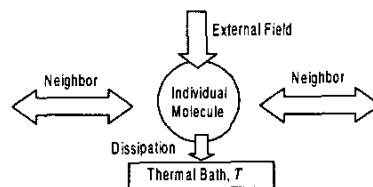


Figure 4. Schematic representation of a nanodevice which is exposed to external fields and a heat bath, and which interacts with its neighbors through electric or magnetic fields.

In previous work [4], we have shown that the electronic or magnetic state at time t of any open quantum system can be described by a state-vector, the so-called coherence vector $\lambda(t)$, which represents the Hermitean density matrix of the system. For the case of a two-level system, the coherence vector has three components, which corresponds to a 2-by-2 density matrix.

The electronic dynamics of such a nanostructure may be described by quantum Markovian master equations of finite-state systems. This model describes the dynamics of a device as the irreversible evolution of an open quantum system coupled to a reservoir (heat bath). This coupling to the environment introduces damping terms in the dynamic equations, which then take the general form of:

$$\hbar \frac{d\lambda(t)}{dt} = \Omega\lambda(t) + R\lambda(t) + k$$

Here, Ω is the Bloch matrix of the corresponding conservative (non-dissipative) quantum system, and R and k are the damping matrix and vector, respectively. The details can be found in [4, 5].

The mixed quantum-classical equations describe the time evolution of the state of the nanodevice. The coherence vector determines the electronic evolution within the framework of a density-matrix description, and all experimentally observable quantities are related to its components. For the case of a two-state system, the third component of the vector $\lambda_3(t)$ determines the electronic charge configuration.

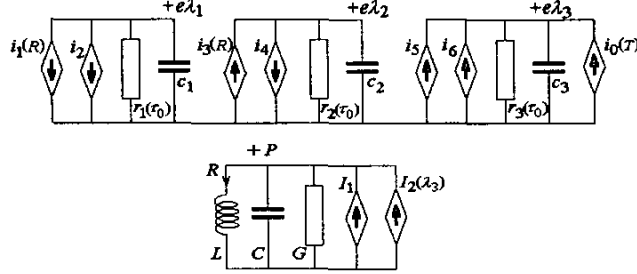


Figure 5. Equivalent-circuit representation of the mixed quantum-classical dynamics for a 2-state nanostructure with one-dimensional nuclear vibration

Notice that the above (ordinary differential) equation resemble circuit dynamics. The equations for the various components of $\lambda(t)$ can be interpreted as the state equations of a nonlinear circuit with state variables λ_1 , λ_2 , and λ_3 . The various terms in the coupled equations can be viewed as nonlinear resistors, capacitors, inductors, and controlled sources. This is schematically shown in Figure 5 above for the case of two-state nanostructure with a 3-dimensional state vector λ .

4 Equivalent-Circuit Models for Coulomb-Coupled Nanodevices

We assume that the individual devices or molecules in an array are fixed in space, and that the electronic dynamics takes place inside each individual molecule (no intermolecular charge transfer). We also assume that the molecules are far enough apart from each other that the overlap between their wave functions can be ignored. We can then identify sets of private electrons and Hamilton operators as belonging to each molecule. Intermolecular forces due to field coupling are relatively weak and their effects can be considered as perturbations.

In order to model the Coulombic interactions between individual molecules, we need to be able to describe the way in which charge is distributed inside each molecule. It is well known that Coulomb interactions between charges localized inside spheres can be specified by the interactions between multipoles (point charges, dipoles, quadrupoles, octopoles, etc.) representing the charge distribution inside the isolated sphere surrounding a molecule.

In this way, the time-varying Coulomb field of an individual molecule can be represented by multipoles at fixed positions with time-varying multipole moments. If the dynamics of a molecule with its time-varying electronic charges are known, then the potential at the site of the neighbor can be determined (and thus the interaction energies). This allows us to model the effects of the neighbors on any individual molecule in the array.

For the equivalent circuit model, the effect of the neighbors is represented by controlled-sources, which are dependent upon the state variable that describes the charge configuration (λ_3 for the case of a 2-state device).

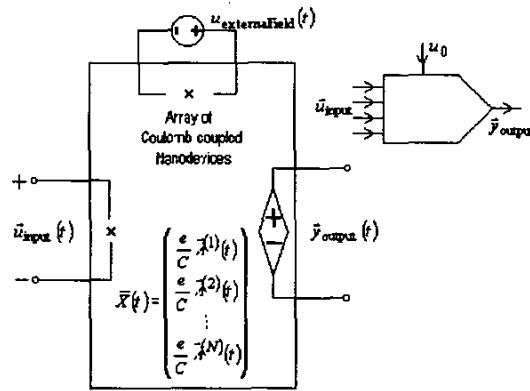


Figure 6. Schematic representation of the equivalent-circuit model for the input and output of an array of field-coupled nanodevices.

Figure 6 below illustrates the equivalent-circuit model of the input and output of an array. As mentioned above, the input is a time-varying electric field generated by a metal-contacted input circuit. Looking back from the array, it can always be represented by a vector of λ_3 's of the nanodevices (I_1, I_2, \dots denote the input ports)

$$\vec{u}_{\text{input}} = \left(\frac{e}{C} \lambda_3^{(i_1)}, \frac{e}{C} \lambda_3^{(i_2)}, \dots \right)$$

The external field will be represented by an independent time-varying voltage source $\vec{u}_{\text{external field}}(t)$. The measured output is also a vector of the λ_3 '-s (O_1, O_2, \dots denote the output ports)

$$\vec{y}_{\text{output}} = \left(\frac{e}{C} \lambda_3^{(o_1)}, \frac{e}{C} \lambda_3^{(o_2)}, \dots \right)$$

Note that e/C , i.e. the electron's charge divided by a capacitance has voltage dimension thus the inputs and outputs are indeed virtual voltages.

4.1 Quantum-Dot Cellular Automata

A concrete example of Coulomb-coupled nanodevices is the *Quantum-Dot Cellular Automata* (QCA) concept [5 – 8]. The Notre Dame proposal is based on a cell which contains five quantum dots, as schematically shown in Fig. 7. The dots are shown as the circles which represent the confining electronic potential. In the ideal case, this cell is occupied by two electrons, which are schematically shown as the solid dots. The electrons are allowed to “jump” between the individual dots in a cell by the mechanism of quantum mechanical tunneling. Tunneling is possible on the nano-meter scale when there is sufficient leaking of the electronic wavefunction out of the confining potential of each dot, and the rate of these jumps may be controlled during fabrication by the physical separation between neighboring dots.

This quantum-dot cell represents an interesting dynamical system. The two electrons experience their mutual Coulombic repulsion, yet they are constrained to occupy the dots. If left alone, they will seek the configuration corresponding to the physical ground state of the cell. It is easy to see that the ground state of the system will be an equal superposition of the two configurations with electrons at opposite corners, as shown in Fig. 7. We may associate a “polarization” of $P=+1$ and $P=-1$ with either arrangement.

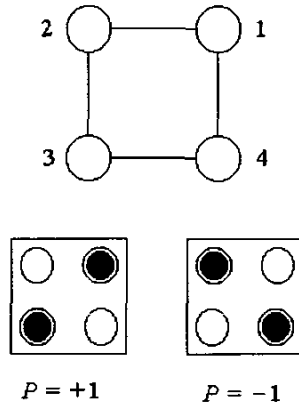


Figure 7. Schematic representation of a quantum-dot cell which is occupied by two electrons.

Coupling between the two cells is provided by the Coulomb interaction between the electrons in different cells. Simulations have shown that this interaction leads to a strongly bistable behavior in that the polarization in one cell induces the same polarization in the neighbor.

This bistable saturation is the basis for the application of such quantum-dot cells for computing structures. The nonlinear saturation replaces the gain in conventional circuits. Note that no power dissipation is required in this case. One can think of the saturation levels of the polarization as the “signal rails.” Based upon the bistable behavior of the cell-cell coupling, the cell polarization can be used to encode binary information. The physical interactions between cells may be used to realize elementary Boolean logic functions [6-9].

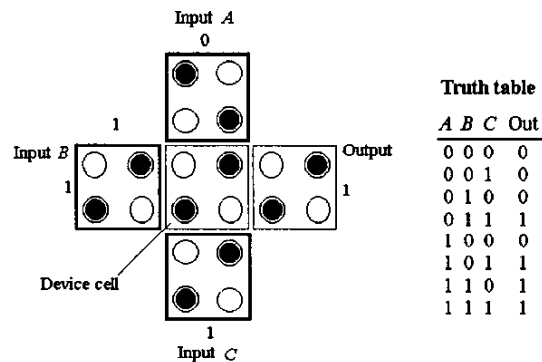


Figure 8. Schematic representation of a majority logic gate built from QCA cells.

Figure 8 above shows a majority logic gate, which is the basic QCA logic gate. It consists of just an intersection of lines and the “device cell” is simply the one in the center. If we view three of the neighbors as inputs (kept fixed), then the polarization of the output cell is the one which “computes” the majority votes of the inputs. Note that conventional AND and OR gates are hidden in the majority logic gate. Inspection of the majority-logic truth table reveals, that if input A is kept fixed at 0, the remaining two inputs B and C realize an AND gate. Conversely, if A is held at 1, B and C realize a binary OR gate. In other words, majority logic gates may be viewed as programmable AND and OR gates.

4.2 Quantum-Dot Cellular Neural Networks

QCA arrays can also be thought of in the framework of *Cellular Neural/Nonlinear Networks* (CNN) [2]. As described in Ref. [13], for the case of a 2-state QCA model, the equivalent circuit describing a CNN cell is composed of two linear capacitors, four nonlinear controlled sources and eight linear controlled sources representing the interactions between the cell and its eight neighbors. This network model simulates the dynamics of the polarization and the phase of the coupled cellular array. If the polarization of the driver cells at the edges of an array initially in equilibrium is changed in time, a dynamics of the polarizations and phases of the cells is launched in the whole array. This dynamics of different arrays has been studied, and a class of spatio-temporal wave-phenomena was identified and explored.

In the framework of the CNN model, ground-state computing by the Quantum Cellular Array corresponds to transients between equilibrium states. Let us assume that in an equilibrium state the configuration of the array is a binary string s . If at $t=0$ the polarization of a few driver cells is abruptly changed from -1 to $+1$ or from $+1$ to -1 , then a transient emerges. If we wait till the new equilibrium is reached, we get a new configuration $f(s)$ of the binary cells. We can say that the array “mapped” s to $f(s)$. In this sense the cellular network model simulates the functions of the quantum-dot cellular automata, including QCA Logic.

5 Equivalent-Circuit Models for Magnetically-Coupled Nanodevices

The behavior of magnetic materials is described by the classical theory of micromagnetism. In large, (micron or bigger) size bulk materials the balance of dipolar coupling and exchange interaction between magnetic moments results in complicated domain structure, experimentally observed and theoretically calculated from the solution of the Landau – Lifshitz equations. In contrary, small (typically 1-50 nm size) magnets exhibit single – domain behavior, i.e. their state is approximately described by a single magnetization vector, and their dynamics governed by ordinary differential equations. If the dots are close to each other, these differential equations are strongly coupled.

Based on these differential equations, we have begun to construct circuit models of nanomagnet arrays and to examine the effect of geometry (dot shape, distance, etc.) on the “circuit” parameters [11]. These circuit models make the design of larger structures rather straightforward, and by using them, one can then analyze realization issues of larger systems (i.e. error tolerance, ease of design, simplest models); this work is in progress. Our goal is to show that the bistable behavior of anisotropic dots (such as magnetic pillars) can be utilized for building binary Boolean logic gates, very much like its electrical QCA counterpart.

5.1 Single-Domain Magnetic Nanoparticles

Our circuit models are based on the single-domain approximation, which generally applies to magnetic particles with sizes on the sub-micrometer regime. Before building models of more complex systems, we shall now verify the single-domain approximation and remark on its limitations.

Single-domain behavior is not a well-defined concept. “Perfectly” single domain particles are sub-10 nm size, and therefore hard to fabricate, and they show superparamagnetic behavior at room-temperature. Nearly-single-domain permalloy particles are typically under 150 nm in size. They show some inhomogeneities of magnetization, especially during switching reversal and if their shape is elongated (so called nonuniform rotation). Fortunately, their behavior still can be understood in the framework of the single-domain approximation, but for higher accuracy the parameters should be fitted to more complex simulations or measurements. Figure 9 below illustrates the magnetization distribution and reversal behavior of such a particle. A single-domain fit is also plotted, demonstrating the validity of the single-domain approximation in this case.

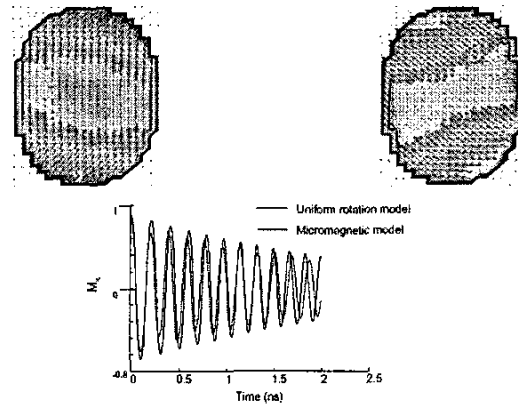


Figure 9. Transient behavior of a *near*-single domain magnetic particle with major axis of 150nm. The figure shows a comparison between the full micromagnetic theory and the single-domain approximation.

Elongated particles with major axis below $1\mu\text{m}$ show single-domain behavior in the remanent state, but split into domains during reversal. The single-domain model is not applicable to the dynamics, but the behavioral and the precession-free models may be used to determine the magnetization behavior under slowly-varying external fields.

5.2 Coupled Magnetic Nanoparticles

We will examine applications of coupled nano-magnets, but first we introduce the two basic types of coupling.

Horizontal coupling occurs in a 1D (line) structure of magnets if the direction of coupling is parallel to the easy axis (the preferred direction of magnetization), which is the long axis. In this case, the lowest-energy state occurs if all the magnets are aligned parallel (ferromagnetic ordering). A schematic of this coupling is shown in Figure 10 below.



Figure 10. Ferromagnetic coupling between nanoparticles.

On the other hand, antiferromagnetic coupling occurs, when the easy axis is perpendicular to the direction of coupling. A schematic of this type of coupling is shown in Figure 11 below.

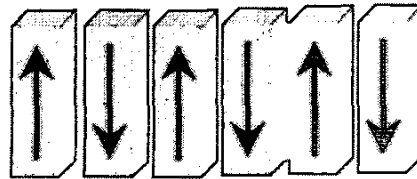


Figure 11. Antiferromagnetic coupling between vertical magnetic nanoparticles (pillars).

Experimental AFM and MFM images of coupled magnetic dots are shown in Figure 12 below. The topographic data (AFM images of the dots) is shown in the top row, the magnetic images are shown in the middle (MFM data), and the bottom row shows a schematic drawing of the magnetization directions.

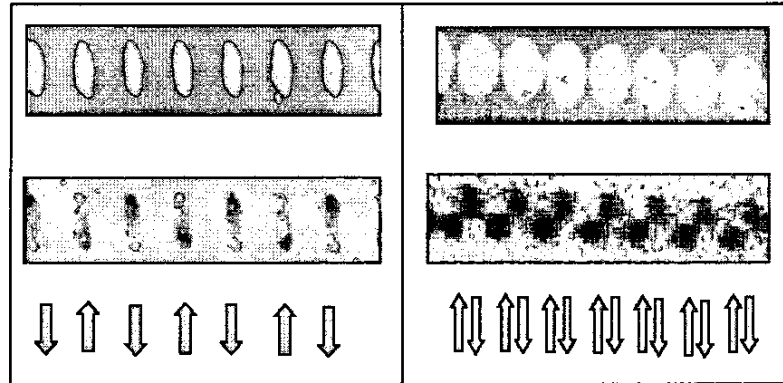


Figure 12. Experimental AFM and MFM images of coupled magnetic dots

5.3 Adiabatic Control of Magnetic Ordering : The Clocked Nanowire

A critical issue for the application of coupled nanomagnets is controlled switching dynamics. We will show that it is possible to control the ordering by slowly-varying external fields, which allows to transition a nanomagnet structure into a well-defined final state.

As an example, we show the adiabatically-pumped magnetic nanowire, which consists of a line of magnetic dots (schematically shown in Figure 13 below) and exposed to an external pumping field. The Figure shows several instances during the pumping cycle. An increasing, and then decreasing magnetic field is applied along the line of dots, and the strength of this field is proportional to the length of the arrow shown in the figure below. Micromagnetic simulations were used to demonstrate the adiabatic switching cycle.

The line is assumed to be in some initial state (a). In the first phase (b), a very strong field is applied which is able to switch every dot, except the input dot, which has a higher switching field (due to its shape). By the end of this first phase, the “memory” of the structure is erased; the magnetic moments of the wire dots are in line with the strong external field, regardless of their previous state. In the second phase (c), this external field is slowly released, and the moments order according to the state of the first dot, which retained its magnetization. The final state (d) corresponds to the correct antiferromagnetic ordering.

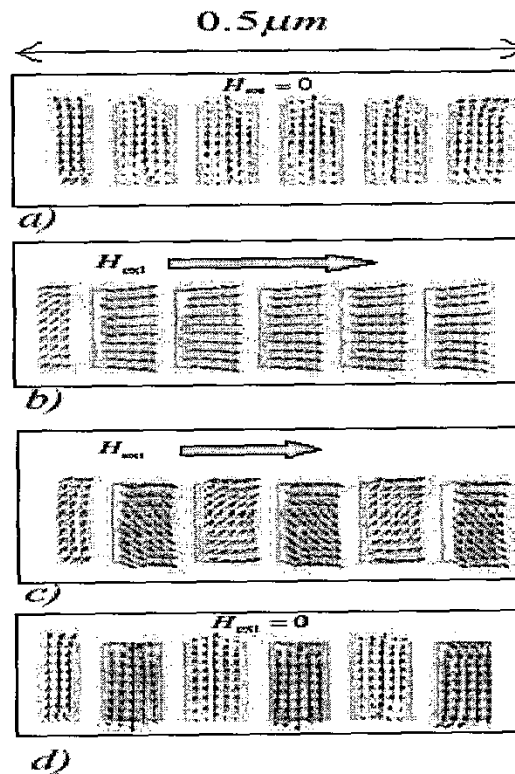


Figure 13. Micromagnetic simulations of the adiabatic pumping cycle of a line of magnetic dots, which represent a magnetic nanowire.

The term ‘adiabatic control’ is used since the dots always remain close to their ground state during the switching phase. As no precession of the magnetization vector occurs, complicated nonlinear dynamics are suppressed. If we can make sure, that the switching “kink” propagates from the first dot to the left, and each dot switches only after its left neighbor did so, then the ordering will be perfect. This will be the case if the switching fields of the dots are exactly the same.

This nanowire is easily modeled in the single-domain approximation, which allows an equivalent-circuit representation for the process. Without going into the details, the results of a SPICE simulation for the magnetic nanowire are shown in Figure 14 below. The wire parameters and phases (a) – (d) are the same as in Figure 13.

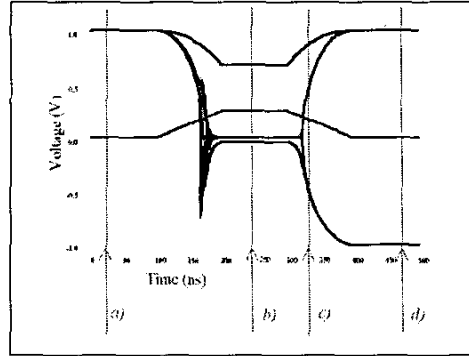


Figure 14. Equivalent-circuit model results for a nanowire within the single-domain SPICE model. The stages *a*), *b*), *c*), *d*) corresponds to the micromagnetic simulation in Figure 13.

Since large, regular matrices of nanomagnets are relatively easy to realize (unlike the irregular arrays), Boolean logic (which requires irregular geometry) probably is not the most natural way of exploiting magnetic nanocomputing. Therefore, we are examining pattern formation phenomena in nanomagnet arrays, for their application possibilities for non – Boolean computation. Our preliminary simulations so far suggest that nanomagnet arrays appear to be excellent candidates for experimentally studying, designing and utilizing complex, nonlinear phenomena in large-scale systems.

6 Discussion

In this paper, we have reviewed our approach for the simulation of field-coupled devices. We have developed equivalent-circuit representations for the dynamics of arrays of field-coupled (electric and magnetic devices), as well as for their interconnection with more conventional metal-contacted devices. This approach yields circuit models, which can be implemented in conventional circuit-simulation tools, and can be used to aid circuit design. We have already demonstrated the feasibility of the co-simulation of field-coupled devices with conventional CMOS devices and single-electron transistors [14].

Acknowledgements

This work was supported in part by grants from the U.S. Office of Naval Research (MURI program) and the W. M. Keck Foundation.

References

- [1] H. Rohrer (1986 Nobel Prize winner in Physics), *Nanotechnology: back to the future of mechanics*, Plenary talk at the IEEE International Symposium of Circuits and Systems, ISCAS 2000, Geneva, 28-31 May 2000.
- [2] S. C. Minne, G. Yaralioglu, S. R. Manalis, J. D. Adams, J. Zesch, C. F. Quate, *Automated parallel high speed atomic force microscopy*, *Applied Physics Letters*, Vol 72, No. 18, pp. 2340-2342 (1998).
- [3] A. I. Csurgay and W. Porod, Equivalent Circuit Representation of Arrays Composed of Coulomb-Coupled Nanoscale Devices: Modeling, Simulation, and Realizability, *International Journal of Circuit Theory and Applications*, 29: 3-35 (2001).
- [4] A. I. Csurgay W. Porod, and C. S. Lent, Signal Processing with Near-Neighbor-Coupled Time-Varying Quantum-Dot Arrays, *IEEE Trans. CAS I* 47(8): 1212-1223 (2000).
- [5] C. S. Lent, P. D. Tougaw, W. Porod, and G. H. Bernstein, Quantum Cellular Automata, *Nanotechnology* 4: 49-57 (1993).
- [6] W. Porod, Computing with Coupled Quantum Dots: Quantum-Dot Cellular Automata and Cellular Nonlinear Networks, *Proceedings of the ECCTD'97*, 248-253 (1997).
- [7] C. S. Lent and P. D. Tougaw, A device Architecture for Computing with Quantum Dots, *Proceedings of the IEEE*, 85: 541 (1997).
- [8] G. L. Snider, A. O. Orlov, R. K. Kumamuru, R. Ramasubramaniam, I. Amlani, G. H. Bernstein, C. S. Lent, J. L. Merz, and W. Porod, Quantum-dot Cellular Automata: Introduction and Experimental Overview, *Proceedings of the First IEEE Conference on Nanotechnology*, Maui, Hawaii, 2001.
- [9] R. P. Cowburn and M. E. Welland, Room Temperature Magnetic Quantum Cellular Automata, *Science* 287: 1466 (2000).
- [10] G. Csaba and W. Porod, Computing Architectures for Magnetic Dot Arrays, presented at the *First International Conference and School on Spintronics and Quantum Information Technology*, Maui, Hawaii, May 2001.
- [11] D. K. Ferry and W. Porod, Interconnections and architecture for ensembles of microstructures, *Superlattices and Microstructures*: 2, 41 (1986).
- [12] L. O. Chua and L. Yang, Cellular Neural Networks: Theory, *IEEE Trans. CAS*, 35: 1257-1272 (1998); Cellular Neural Networks: Applications, *ibid.* 1273-1290 (1998).
- [13] CNN Software Library (Templates and Algorithms) V 7.2, Analogical and Neural Computing Laboratory, Computer and Automation Institute, Hungarian Academy of Sciences, 1998.
- [14] C. Gerousis, X. Wang, G. Toth, S. M. Goodnick, W. Porod, C. S. Lent, and A. I. Csurgay, Modeling Nanoelectronic CNN Cells: CMOS, SETs and QCAs, *Proceedings of the IEEE International Symposium on Circuits and Systems*, Geneva, May 2000.